Line Tension Effects near First-Order Wetting Transitions

J. Y. Wang, S. Betelu,* and B. M. Law

Condensed Matter Laboratory, Department of Physics, Kansas State University, Manhattan, Kansas 66506-2601

(Received 17 May 1999)

The behavior of the line tension for *n*-octane or 1-octene droplets on a hexadecyltrichlorosilane coated Si wafer, near a first-order wetting transition, qualitatively agrees with the theoretical predictions of Indekeu [Physica (Amsterdam) **183A**, 439 (1992)] and the calculations of a number of other groups. A simple phenomenological model possessing a repulsive barrier at $l_0 = (5.1 \pm 0.2)$ nm and a horizontal correlation length $\xi = (0.40 \pm 0.03)$ μm provides a quantitative description of the experiments.

PACS numbers: 68.45.Gd, 68.10.Cr, 82.65.Dp

An understanding of surface phase transitions and the wettability of surfaces has been of much recent interest due to the desire to engineer surfaces with specific characteristics. Undoubtably the most widely studied surface phase transition is the wetting transition which can be either first [1] or second order [2]. In first-order wetting transitions, a macroscopic droplet of contact angle θ_∞ situated on a solid surface is in mechanical equilibrium with an adsorbed film of microscopic thickness l_1 [Fig. 2, inset (below)]. As the temperature is increased towards the wetting temperature T_w, the contact angle θ_∞ approaches zero, however, the thickness l_1 remains finite until T_w whereupon it increases *discontinuously* to a large (and perhaps macroscopic) value. For second-order wetting transitions, as the temperature is increased towards T_w, the thickness l_1 increases *continuously* to a large and perhaps macroscopic value above T_w. The difference in behavior for first- and second-order wetting transitions is governed by the shape of the free energy per unit area $V(l)$ as a function of the film thickness l as T_w is approached [3]. In this paper, we are interested in first-order wetting transitions which are the most common in nature. For temperatures $T < T_w$, the potential $V(l)$ has the generic shape depicted in Fig. 1 (inset). The surface energy of the adsorbed film σ_{sv} of thickness l_1 is less than that of a thick film (or droplet) of energy $\sigma_{sl} + \sigma_{lv}$ (for $l \to \infty$) and an energy barrier exists between the *global* minimum at l_1 and the local minimum at $l \to \infty$. As the temperature is increased towards T_w, the surface energies σ_{sv} and $\sigma_{sl} + \sigma_{lv}$ become more similar in magnitude until at T_w, where $\theta_\infty = 0°$, Antonow's rule holds [4] and $\sigma_{sv} = \sigma_{sl} + \sigma_{lv}$ so that the two minima now have identical energies. For $T > T_w$, the surface energy $\sigma_{sv} > \sigma_{sl} + \sigma_{lv}$ and the minimum at l_1 is now a local rather than a global minimum. This type of transition is conveniently expressed in terms of the spreading coefficient $S = \sigma_{sv} - \sigma_{sl} - \sigma_{lv}$ which is negative for $T < T_w$ and becomes equal to zero at T_w.

Unfortunately very little is known about the precise shape of $V(l)$ at small l except that it is expected to possess the generic form displayed in Fig. 1 (inset). Our understanding of $V(l)$ is improved at large l where the shape is governed by long-range dispersion interactions with $V(l) \sim W/l^{(\sigma-1)}$ where the Hamaker constant W (>0 for first-order wetting) depends upon the materials properties of the system while $\sigma = 3$ (4) for nonretarded (retarded) interactions [5]. Recent theoretical work [6] suggests that a measurement of the line tension τ, namely, the energy per unit length associated with the three-phase solid/liquid/vapor contact line of a liquid droplet situated on a solid surface, will provide valuable experimental insight into the behavior of $V(l)$ near T_w. Later in this paper, we present the first experimental study of τ near a wetting transition; however, before presenting these results we summarize the theoretical predictions for τ in this region.

There has been considerable theoretical debate concerning the predicted behavior of τ in the vicinity of a wetting transition because differing theoretical results suggest that τ is either zero, finite, or diverges to infinity at T_w [6–8].

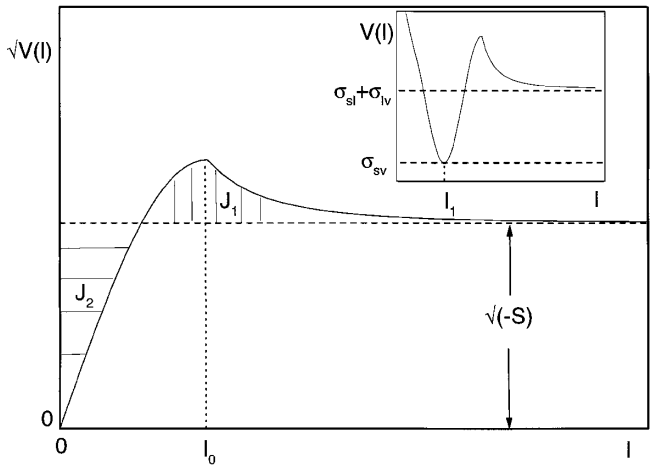

FIG. 1. Plot of $\sqrt{V(l)}$ as a function of thickness l for the potential described by Eqs. (6) and (7) where a repulsive barrier exists at l_0. The areas J_1 and J_2 [Eq. (2)] are shaded while the adsorption minimum has been shifted to the origin. The generic shape of the potential $V(l)$ for $T < T_w$ is shown in the inset. The adsorption film of thickness l_1 has a lower energy σ_{sv} than a thick film or droplet at $l \to \infty$ with energy $\sigma_{sl} + \sigma_{lv}$.

A consensus now seems to have been reached concerning the behavior of τ near T_w, which is nicely summarized in [9]: the behavior of τ near T_w depends upon both the order of the wetting transition and also the range of the surface interactions. For first-order wetting transitions the line tension is predicted to exhibit certain universal features which can most easily be understood via a geometric interpretation due to Indekeu [6]. According to his interface displacement model,

$$\tau = \sqrt{2}\,\sigma_{lv}\xi \int_0^\infty dx[\sqrt{V(x)/\sigma_{lv}} - \sqrt{-S/\sigma_{lv}}\,], \quad (1)$$

$$= \sqrt{2\sigma_{lv}}\,\xi[J_1 - J_2], \quad (2)$$

J_1 and J_2 are the shaded areas in Fig. 1 which provide a convenient connection between the shape of $[V(x)]^{1/2}$ and τ, the correlation length ξ is a characteristic length along the substrate, while x is a dimensionless film thickness (defined more precisely later). In Fig. 1, the adsorption minimum has been shifted to the origin. Sufficiently far from T_w the magnitude of τ is predicted to be of order $\sim 10^{-12}$ to 10^{-10} N [4,10]. The thermal variation of τ is governed by the integral in Eq. (1) which depends upon temperature T through the contact angle θ_∞ which is related to S [see Eq. (4) below]. In many of the theoretical calculations for τ [6,8,10], the area J_2 dominates J_1 sufficiently far from T_w so that τ is negative; however, on approaching T_w the spreading coefficient $S \to 0$ and therefore the area $J_2 \to 0$, hence, τ is *positive and perhaps infinite* depending upon the area J_1 at T_w. This positivity at T_w is a consequence of the repulsive barrier between the two minima at l_1 and $l \to \infty$ in the potential $V(x)$. Indekeu [6] has demonstrated that

$$\tau = \tau_0 - \tau_1 X, \quad (3)$$

where X takes the form $t^{1/2}\ln(1/t)$ for short-range (SR) interactions, $\ln t$ for nonretarded long-range (NLR) interactions, and $t^{1/6}$ for retarded long-range (RLR) interactions, the reduced temperature $t = (T_w - T)/T_w$, $\tau_1 > 0$ while $\tau_0 = \tau(t = 0) > 0$ for SR and RLR interactions. For each of these situations, τ changes from a negative to a positive value with increasing absolute slope $|d\tau/dt|$ as T_w is approached. At T_w, τ is positive and finite for SR and RLR interactions while it is infinite for NLR interactions.

In this contribution, we use microscopic interferometry to study the behavior of the line tension τ near a first-order wetting transition. For very large droplets, the contact angle θ_∞ is related to the surface energies σ_{ij} between bulk phases i and j via the Young-Dupré equation [4]:

$$\cos\theta_\infty = \frac{\sigma_{sv} - \sigma_{ls}}{\sigma_{lv}} = 1 + \frac{S}{\sigma_{lv}}, \quad (4)$$

where $s \equiv$ solid, $l \equiv$ liquid, and $v \equiv$ vapor. For small droplets, the contact angle θ will differ appreciably from its large radius limit θ_∞ because line tension effects become important. For finite lateral radii r (Fig. 2, inset), the contact angle θ is described by the modified Young-Dupré equation [11:

$$\cos\theta = \cos\theta_\infty - \frac{\tau}{r\sigma_{lv}}, \quad (5)$$

and therefore a study of $\cos\theta$ versus $1/r$ allows us to determine the magnitude and sign of τ.

We have chosen to study n-octane and 1-octene droplets on self-assembled monolayers (SAMs) of hexadecyltrichlorosilane coated (100) Si wafers which exhibit a wetting transition temperature at, respectively, $T_w = 45.4$ and 51.2 °C (Fig. 3). The SAM monolayers were prepared on these wafers using standard wet chemistry procedures [12,13]. Both the oxide covered Si wafers and the SAM coated Si wafers had a surface roughness of ~0.5 nm measured using an atomic force microscope in contact mode. The contact angle hysteresis on the SAM monolayer was ~1°, in agreement with the best wafers prepared by [12], while T_w varied by no more than ~1 °C for droplets on differing wafers or for droplets on the same wafer. From the wetting temperatures for octane and octene, we obtain critical surface tensions of $\sigma_c = 19.2$ and 18.7 mJ/m^2, respectively, where the former value is in reasonable agreement with 20.5 ± 0.5 mJ/m^2 from [12]. The variability of 1 °C in T_w gives $\Delta\sigma_c = 0.1$ mJ/m^2 which indicates that the SAMs exhibit excellent reproducibility and a low surface heterogeneity of $\Delta\sigma_c/\sigma_c \approx 0.005$. Droplets of variable size were formed on the SAM covered Si wafer using a two-stage oven. An outer heater stage determined the temperature of a bulk liquid reservoir while an inner thermoelectrically cooled stage, on which the Si wafer

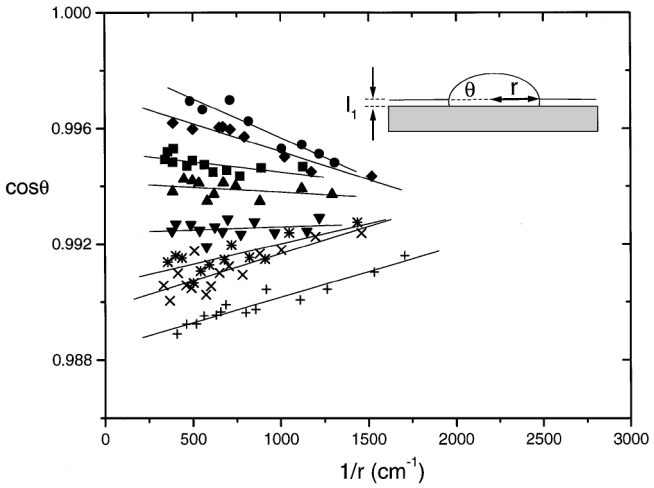

FIG. 2. Plot of $\cos\theta$ versus $1/r$ for droplets of 1-octene on a hexadecyltrichlorosilane coated Si wafer at various temperatures $T = 40.7$ (plusses), 42.1, 43.1, 44.0, 46.0, 47.3, 48.6, and 50.0 °C (solid circles). The solid lines are a linear fit to the data. In the inset, we schematically show a droplet of contact angle θ and lateral radius r in mechanical equilibrium with an adsorbed layer of thickness l_1.

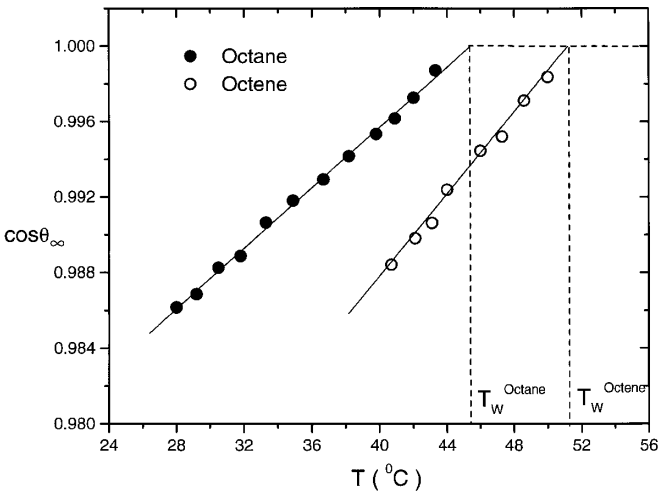

FIG. 3. Plot of $\cos\theta_\infty$ as a function of temperature T for octane and octene. The solid lines are linear fits to the data while the wetting temperatures T_w correspond to $\cos\theta_\infty = 1$.

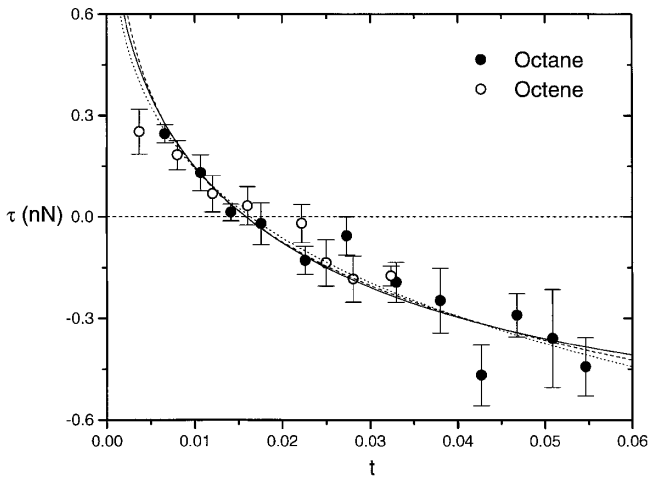

FIG. 4. Line tension τ as a function of the reduced temperature $t = (T_w - T)/T_w$ for octane and octene. The solid, dashed, and dotted lines are fits to the octane data for short-ranged, nonretarded long-ranged, and retarded long-ranged interactions, respectively, using Eq. (3). If the octane data is fitted with the nonretarded model in Eqs. (6) and (7), this model gives a curve identical to the dashed line where $W_0 = 0.0018$ and $\sigma_{lv}\xi = 8.3 \times 10^{-9}$ N.

was situated, allowed droplets to be condensed at a sufficiently slow rate so that dynamic contact angle effects were unimportant [14]. Advancing contact angles were measured as a function of radius r with $r \sim 5$–$100\ \mu$m for temperature differences $\Delta T = T_w - T \sim 1$–$10\,^\circ$C. Monochromatic illumination of the droplet created interference fringes which were observable under a microscope. By fitting the interference fringes to a spherical cap shaped droplet the contact angle θ and the lateral radius r could be accurately determined; a plot of $\cos\theta$ versus $1/r$ allowed τ and $\cos\theta_\infty$ to be determined from the slope and intercept, respectively [Eq. (5)]. In Fig. 2 we show such a plot for octene at various temperatures. The slope changes continuously from a positive to a negative value with increasing temperature and therefore τ changes from a negative to a positive value on approaching T_w. In Fig. 3 we have plotted $\cos\theta_\infty$ versus T for both liquids. The characteristic discontinuity in the slope $d\cos\theta_\infty/dT$ at T_w is an indication that the wetting transition is indeed first order [1] as required and therefore $V(l)$ should possess the characteristic shape depicted in Fig. 1 (inset).

In Fig. 4 we have plotted τ versus t for octane (solid circles) and octene (open circles). Both liquids exhibit almost identical behavior as a function of t. The overall behavior in Fig. 4 agrees with many of the predictions in [6,8,9], specifically, for increasing temperatures towards T_w, τ changes from a negative to a positive value with increasing absolute slope $|d\tau/dT|$. The positive value of τ at T_w implies that an energy barrier exists between the two minima at l_1 and $l \to \infty$ [Eq. (1) with $S = 0$]. The experimental data also agree with the predictions from Eq. (3), however, the experimental resolution for τ and the range in ΔT are insufficient to determine whether short-range or nonretarded/retarded long-range interactions make the dominant contribution to τ. The solid, dashed, and dotted lines represent fits to the octane data for, respectively, short-ranged, nonretarded long-ranged, and retarded long-ranged interactions with τ_0 and τ_1 as adjustable parameters. All three curves provide an equally good description of the experimental data. There are also some striking differences between the theoretical calculations, for various models of $V(\ell)$, and the experimental results: (i) the magnitude of τ is at the upper limit predicted by theory [4,10], and (ii) for many of the models considered by various authors [6,8,10] the line tension changes sign at large contact angles $\theta_\infty \sim 60^\circ$ or correspondingly at low temperatures $\Delta T \sim 30\,^\circ$C far below T_w. In contrast, the experiments for both octane and octene find that τ changes sign close to T_w at $t = 0.016$ corresponding to $\theta_\infty(\tau = 0) = 5.0^\circ$. The experimental quantity $\theta_\infty(\tau = 0) = 5.0^\circ$ provides important microscopic information about the shape of the potential $V(l)$ because this quantity is determined by the integral in Eq. (1), independent of the magnitude of $\sigma_{lv}\xi$, and occurs when the areas $J_1 = J_2$ in Fig. 1.

What does $\theta_\infty(\tau = 0) = 5.0^\circ$ tell us about the shape of $V(l)$? In order to examine this question we consider a phenomenological potential in the same spirit as [6]. Specifically, we consider the following dimensionless potential:

$$V(x)/\sigma_{lv} = A(1)[1 - \cos(\pi x)]/2, \quad 0 \le x < 1, \tag{6}$$

$$= A(x), x \ge 1, \tag{7}$$

in the integrand of Eq. (1), where $A(x) = W_0/x^2 - S/\sigma_{lv}$, $W_0 = W/\sigma_{lv} l_0^2$, and the dimensionless length

$x = l/l_0$. This potential possesses the necessary generic features expected for $V(x)$: it is a harmonic potential ($\sim l^2$) at $l \ll l_0$ with a repulsive barrier at $l \sim l_0$, while for large $l \gg l_0$ it exhibits a nonretarded interaction $V(l) \sim W/l^2 - S$ which correctly decays to $-S$ at very large $l \to \infty$ (Fig. 1). The spreading coefficient S in this potential is related to θ_∞ [Eq. (4)] and T (using Fig. 3), W is a constant for a particular system, and the *shape* of the potential and the *height* of the repulsive barrier is controlled by the length l_0. There are two independent length scales in our model for τ: l_0 which controls the contact angle $\theta_\infty(\tau = 0)$ and ξ which controls the absolute magnitude of τ. In order to compare our model with experiment, τ was calculated using Eqs. (1), (6), and (7), where $W_0(= 0.0018)$ was adjusted to provide agreement with the measured value of $\theta_\infty(\tau = 0)$, while $\sigma_{lv}\xi(= 8.3 \times 10^{-9}$ N) was adjusted to provide the correct magnitude for τ. The results for τ as a function of t agree with the dashed line in Fig. 4, obtained previously using Eq. (3) for NLR interactions. This model therefore provides a good description of the experiments. Both octane and octene possess a $W \approx 1.0 \times 10^{-21}$ J [5] and $\sigma_{lv} \approx 20.7$ mJ/m^2; we therefore find that $l_0 = (5.1 \pm 0.2)$ nm and $\xi = (0.40 \pm 0.03)$ μm. The position of the repulsive barrier at $l_0 = 5.1$ nm is in reasonable agreement with the repulsive barrier measured for liquids between two mica plates in the surface forces apparatus of Israelachvili [5]. The horizontal length scale $\xi = 0.4$ μm determines the magnitude of the line tension τ. Our line tension results are of similar magnitude to a number of other groups [11] and are among the smallest values for liquid droplets situated on flat solid surfaces. There is a wide variability in magnitude for τ [11]. We speculate that this variability could be controlled by factors such as the surface roughness/chemical heterogeneity of the substrate which is often not well characterized. The length ξ would then correspond to the heterogeneity correlation length [15]. A $\xi = 0.4$ μm is not unreasonable for SAM covered Si wafers [16], however, these speculations are in need of further experimental work.

In summary, we have used microscopic interferometry to study the behavior of the line tension τ for small droplets of n-octane or 1-octene on a hexadecyltrichlorosilane coated Si wafer surface in the vicinity of a first-order wetting transition. The experimental measurements are in qualitative agreement with the interface displacement model of Indekeu [6] and theoretical calculations of others [8,10] which predict that the line tension should change from a negative to a positive value with increasing (negative) slope as the wetting transition temperature T_w is approached. The change in sign of τ with temperature and the positive value for τ at T_w is a direct consequence of the presence of a repulsive barrier in the interface potential $V(l)$ for a first-order wetting transition. Our measurements cannot yet distinguish whether the short-range or long-range interactions make the dominant contribution to the line tension, however, by considering a simple phenomenological model which possesses many realistic features we have identified two length scales: (i) $l_0 = (5.1 \pm 0.2)$ nm [corresponding to the position of the repulsive barrier in the potential $V(l)$] which is required in order to explain the condition that $\tau = 0$ when the contact angle $\theta_\infty = 5.0°$, and (ii) a horizontal correlation length $\xi = (0.40 \pm 0.03)$ μm which determines the magnitude of the line tension τ. It is not yet understood why ξ is macroscopic rather than microscopic as expected from theory.

Acknowledgment is made to the donors of the Petroleum Research Fund, administered by the American Chemical Society, and to the National Science Foundation through Grant No. DMR-9631133 for support of this research.

*Present address: School of Mathematics, University of Minnesota, Minneapolis, MN 55455.

[1] J. W. Schmidt and M. R. Moldover, J. Chem. Phys. **79**, 379 (1983).
[2] K. Ragil *et al.*, Phys. Rev. Lett. **77**, 1532 (1996).
[3] P. G. de Gennes, Rev. Mod. Phys. **57**, 827 (1985).
[4] J. S. Rowlinson and B. Widom, *Molecular Theory of Capillarity* (Clarendon, Oxford, 1982).
[5] J. N. Israelachvili, *Intermolecular and Surface Forces* (Academic, London, 1992), 2nd ed.
[6] J. O. Indekeu, Physica (Amsterdam) **183A**, 439 (1992).
[7] N. V. Churaev *et al.*, J. Colloid Interface Sci. **89**, 16 (1982); J. F. Joanny and P. G. de Gennes, *ibid.* **111**, 94 (1986); B. Widom and A. S. Clarke, Physica (Amsterdam) **168A**, 149 (1990); B. Widom and H. Widom, *ibid.* **173**, 72 (1991); C. Varea and A. Robledo, Phys. Rev. A **45**, 2645 (1992); T. Getta and S. Dietrich, Phys. Rev. E **57**, 655 (1998).
[8] I. Szleifer and B. Widom, Mol. Phys. **75**, 925 (1992); H. T. Dobbs and J. O. Indekeu, Physica (Amsterdam) **201A**, 457 (1993); E. M. Blokhuis, Physica (Amsterdam) **202A**, 402 (1994); S. Perković *et al.*, J. Chem. Phys. **102**, 400 (1995); C. Bauer and S. Dietrich, Eur. Phys. J. B **10**, 767 (1999).
[9] J. O. Indekeu, Int. J. Mod. Phys. B **8**, 309 (1994).
[10] H. Dobbs, Langmuir **15**, 2586 (1999).
[11] J. Drelich, Colloids Surf. A **116**, 43 (1996).
[12] J. B. Brzoska, I. Ben Azouz, and F. Rondelez, Langmuir **10**, 4367 (1994).
[13] S. R. Wasserman, Y.-T. Tao, and G. M. Whitesides, Langmuir **5**, 1074 (1989).
[14] In our experiments, the capillary number Ca $\sim 10^{-8}$. Dynamic contact angle effects are observable for Ca $\gg 10^{-5}$ [E. B. Dussan V., Annu. Rev. Fluid Mech. **11**, 371 (1979)].
[15] M. O. Robbins and J. F. Joanny, Europhys. Lett. **3**, 729 (1987).
[16] E. L. Decker and S. Garoff, J. Adhesion **63**, 159 (1997).